Supplementary Material

I) Supplementary Methods (Expanded Methods Section)

II) Supplementary References

III) Supplementary Figures

IV) Supplementary Tables

I) Supplementary Methods (Expanded Methods Section)

Study design

Three different groups of animals ($Kit^{+/+}$ mice, Kit^{W}/Kit^{W-v} mice and Kit^{W}/Kit^{W-v} mice treated with c-kit^{+} bone marrow cells, referred to as $Kit^{+/+}$ BM $\rightarrow$ Kit^{W}/Kit^{W-v} mice) were studied at three different time points (6h, 24h, 7 days) after ischemia-reperfusion injury (Supplementary Figure 1A/B). Mice were investigated *in-vivo* with FMT-XCT. After imaging the mice were sacrificed at each time point for *ex-vivo* analysis by cryoslicing and histology/immunohistochemistry. Additionally, mice injected *in-vivo* with the molecular apoptosis sensor were studied after sacrifice at each time point by flow cytometry. A subgroup of mice was followed with cardiac Magnetic Resonance Imaging (MRI) until day 21 post MI to assess the development of heart function, respectively cardiac failure with subsequent Triphenyltetrazolium-Chloride (TTC) staining for determination of infarct size (for schematic of the study protocol see Supplementary Figure 1C).

Mice

All three groups of mice were on a WBB6F$_1$ background. *Kit* mutant Kit^{W}/Kit^{W-v} mice possess pleiotropic defects in pigment-forming cells, germ cells, RBC's and mast cells, however have a relatively normal live span. In addition, they exhibit an intrinsic progenitor cell defect. The Kit^{W}/Kit^{W-v} mouse is the only c-kit mutant in which mobilization of HSPCs is defective in spite of relatively normal numbers of HSPCs. While the *W* mutation results from a 78-amino acid deletion which includes the transmembrane domain of the c-kit protein, the *W-v* mutation represents a missense mutation in the kinase domain of the c-kit coding sequence[1-3].

Ischemia-reperfusion injury

Myocardial Infarction was induced by transient ligation of the left anterior descending artery (LAD) for 30 minutes with subsequent reperfusion, as previously described [4]. Myocardial infarction was performed in Kit^{W}/Kit^{W-v} mice (n=37), corresponding wild-type $Kit^{+/+}$ mice (n=36) and treated $Kit^{+/+}$ BM $\rightarrow$ Kit^{W}/Kit^{W-v} mice (n=34) (Supplementary Figure 1).

Mice were anesthetized for all surgical and imaging procedures by general inhalation anesthesia (isofluorane 1.5 to 2.5% vol., plus 2 l O_2). After completion of the imaging study mice were sacrificed under deep anesthesia and the hearts were excised and processed for further *ex-vivo* analysis. All animal experiments were approved by the local subcommittee on Research Animal Care (Protocol Number 79-09) and carried out in accordance with the Guide for the care and Use of Laboratory Animals published by the U.S. National Institutes of Health (NIH publication No. 85-23, revised 1996).

Cell therapy with c-kit^{+} bone marrow cells

Mutant Kit^{W}/Kit^{W-v} mice were injected under aseptic conditions with 10^{7} fresh bone marrow cells obtained from $Kit^{+/+}$ donors. Successful population of the heart was confirmed by flow cytometry (Supplementary Figure 2). While Kit^{W}/Kit^{W-v} mice almost lack c-kit^{+} cells in the heart, 6-8 weeks after cell therapy a significant repopulation of c-kit^{+} cells can be detected. The amount of c-kit^{+} cells within the heart was comparable between wild-type $Kit^{+/+}$ mice and treated $Kit^{+/+}$ BM $\rightarrow$ Kit^{W}/Kit^{W-v} mice. After myocardial infarction a slightly higher percentage of c-kit^{+} cells are found within the heart compared to naïve mice without MI (p=0.014, 2-way ANOVA). $Kit^{+/+}$ BM $\rightarrow$ Kit^{W}/Kit^{W-v} mice were used for experiments 10 weeks after therapy with c-kit^{+} bone marrow cells.

Fluorescence Molecular Tomography/X-ray Computed Tomography

In–vivo imaging was performed under inhalation anesthesia with hybrid FMT-XCT. The hybrid FMT-XCT system is a combination of a Fluorescence Molecular Tomography system consisting mainly of a 750nm diode laser (B&W tek) and a Charge Coupled Device (CCD) camera in trans-illumination set-up, and a micro-CT system (General Electric), both mounted on the same 360° rotating gantry[5]. XCT imaging was performed with a tube voltage of 60kV and a tube current of 450μA. 400 views were acquired over 360° rotation angle, the exposure time was 400ms. Spatial resolution resulted in an effective isotropic voxel size of 90μm.

The hybrid reconstruction method developed specifically for this modality obtains accurate reconstructions of the fluorescence distribution using XCT based optical attenuation maps to correct for the influence of optical properties per anatomical region in the forward model calculation and XCT based structural prior information in the inversion[6].

During FMT acquisition we scanned a grid of ~21 laser positions across the mouse chest for 18 projection angles of the gantry over the full 360° range. For reconstruction of the fluorescence signal we segmented the X-ray CT volume in anatomical regions: heart, lung, bone, liver and remaining tissue. Optical properties and reconstruction parameters are shown in Supplementary Table 1 and were determined as previously described[6]. Signal quantification was calculated based on the FMT-XCT reconstructions on a voxel-based analysis using the anatomical segmentation of the X-ray CT, by calculating a voxel within the segmented heart region as positive for the injected molecular apoptosis probe if the signal intensity (SI) in the voxel was higher than the mean SI in the heart + two standard deviations. Additionally we calculated the fluorescence ratio (FR) of the maximum fluorescence

SI observed in the infarcted heart over the average background fluorescence SI in the lung.

Molecular Probes

For the detection of apoptosis we used a fluorescent Annexin V based molecular sensor targeting phosphatidylserine (Excitation: 755nm, Emission 772nm, Annexin-Vivo750, Perkin Elmer). 4h prior to FMT-XCT imaging mice were injected with 2nmol fluorescent probe/25g mouse. For contrast enhanced XCT a long circulating CT contrast agent (Exitron Nano 12000, Viscover) was injected immediately prior to imaging (100μl /25g mouse).

Cardiac Function Assessment

Cardiac function was assessed by Magnetic Resonance Imaging using a clinical 1.5T MRI equipment adapted for small animal imaging (Philips Medical Systems, Best, Netherlands). Animals were studied under general inhalation anesthesia lying in a prone position on a 23mm surface coil. Cine Imaging was performed ECG-triggered under free-breathing conditions. After acquisition of scout scans, 1mm thick contiguous short axis slices were acquired perpendicular to the septum using a standard gradient echo sequence. Parameters for cine image acquisition included: field of view 35x35mm, matrix 160x160, slice thickness 1mm, Time of Repetition/Echo Time 18/7.4ms, flip angle 30°, 1 line/RR interval, temporal resolution 18ms, in-plane resolution 220x220μm, number of signal averages 2. An average of 12 cardiac cycles was acquired per slice. Endocardial and epicardial contours both in the end-systolic and end-diastolic phase were tracked for calculation end-systolic volume (ESV), end-diastolic volume (EDV), stroke volume (SV), ejection fraction (EF)

and left ventricular mass. After completion of MRI at day 21 mice were sacrificed and prepared for *ex-vivo* TTC staining.

Cryoslicing

A subgroup of sacrificed mice were frozen to -80°C and embedded in a mixture of O.C.T. (Optimal Cutting Temperature) medium and India Ink. Cryoslice imaging of the mice was performed using a multispectral imaging system[7]. For ~20 transversal slices per mouse, 250μm apart, we acquired planar RGB images and planar fluorescence images using a filtered white light source and a sensitive CCD camera.

Flow Cytometry

To determine the cellular source of the AnnexinVivo750 signal mice injected with the probe were sacrificed and the hearts processed for further analysis by flow cytometry. Infarct tissue and healthy hearts were harvested, minced with fine scissors, and incubated in a cocktail of collagenase I, collagenase XI, DNase I, and hyaluronidase (Sigma- Aldrich) and digested at 37°C for 1 h, as previously described[8]. Cells were then triturated through nylon mesh and centrifuged (15 min, 500 *g,* 4°C). Total cardiac cell numbers were determined with Trypan blue (Mediatech, Inc.). For calculation of total cell numbers in the heart, normalization to tissue weight was performed. The resulting single-cell suspensions were washed with DPBS supplemented with 0.2% (wt/vol) bovine serum albumine and 1% (wt/vol) fetal calf serum and subsequently stained with propidium iodine (to exclude dead cells) and the following antibodies: FITC - cTroponin-T (Clone 7E7, HyTest Ltd.)[9], PE – c-kit (Clone ACK45, BD Bioscience), Pacific Blue CD11b (Clone M1/70, BioLegend) and PE – Caspase 3 (Clone C92-605, BD Bioscience). We excluded lineage positive cells by using antibodies against CD90, CD49b, B220, NK1.1. and

Ly6G (all from BD Bioscience). For the detection of intracellular caspase-3 and cTroponin-T, cells were resuspended in formaldehyde-containing Cytofix/Cytoperm solution (BD Bioscience) and incubated on ice for 20 minutes. Cells were pelleted and washed with BD Perm/Wash (BD Bioscience). Resuspended cells were then incubated with Caspase 3 and cTroponin-T antibody for 30 minutes at room temperature.

Data were acquired on FACS Aria (BD Biosciences) with a 635nm red laser and 755/LP and 780/60 BP filter configuration to detect AnnexinVivo750.

Histology

For histology hearts were frozen in liquid nitrogen immediately after sacrifice and cut into serial coronal sections of 12µm thickness. Slices were stained with either hematoxylin and eosin (H&E), or DAPI and dUTP nick end labeling (TUNEL) for the detection of apoptosis or used for detection of AnnexinVivo750. For detection of cell death a TUNEL reaction stain was performed according to manufacturer's instructions (In-situ cell death detection kit, Roche Diagnostics, Penzberg, Germany). Unfortunately, due to the additional TUNEL staining we lost fluorescence signal for the injected Annexin-Vivo750. Therefore, although contiguous sections were used, a perfect Co-Staining could not be achieved for all time points. Fluorescence images were captured using an Axio Imager Z2 upright microscope system (Carl Zeiss, Oberkochen, Germany). AnnexinVivo750 was detected with a modified Cy 7 filter set (modification: emission filter: 785 LP; AHF Analysetechnik AG, Tübingen, Germany), TUNEL staining with filter set 09 (488009-9901-000, Carl Zeiss), while nuclei were identified with Hoechst 33342 (filter set 01, 488001-9901-000, Carl Zeiss).

Heart Morphometry

For *ex-vivo* assessment of infarct extension and heart geometry, excised hearts were prepared for staining with TTC. Briefly, hearts were cut in 1mm slices using a specialized mouse heart slicer (Zivic Instruments, Pittsburgh, PA), which allows preparation of 1mm thick slices in a short axis orientation perpendicular to the long axis resembling the short-axis views obtained by CT/MRI. Heart slices were then incubated with 1% Triphenyltetrazolium-Chloride solution (37°C, pH=7,4) for 20min followed by formalin fixation (4% paraformaldehyde, 10min, room temperature). Slices were photographed with a high-resolution digital camera and planimetered using Image J software (http://rsbweb.nih.gov/ij/). Sizes of non-ischemic and ischemic area were calculated for each slice to further calculate the volume of infarcted and remote myocardium.

Data Analysis/Statistics

Statistical analysis was performed using GraphPad Prism 5.0a (GraphPad Software Inc., La Jolla, CA). Results are expressed as mean ± SEM or in case of cardiac function assessment as median and range. For multiple group comparisons analysis of variance (ANOVA), either 1-way or 2-way as appropriate, followed by Bonferroni post-hoc test was performed. All statistical test were performed two-sided and p-values <0.05 were considered indicating statistical significance.

II) Supplementary References

1. Fazel S, Cimini M, Chen L, Li S, Angoulvant D, Fedak P, et al. Cardioprotective c-kit+ cells are from the bone marrow and regulate the myocardial balance of angiogenic cytokines. J Clin Invest. 2006; 116: 1865-77. doi:10.1172/JCI27019.
2. Nocka K, Buck J, Levi E, Besmer P. Candidate ligand for the c-kit transmembrane kinase receptor: KL, a fibroblast derived growth factor stimulates mast cells and erythroid progenitors. EMBO J. 1990; 9: 3287-94.
3. Papayannopoulou T, Priestley GV, Nakamoto B. Anti-VLA4/VCAM-1-induced mobilization requires cooperative signaling through the kit/mkit ligand pathway. Blood. 1998; 91: 2231-9.
4. Nahrendorf M, Sosnovik DE, Waterman P, Swirski FK, Pande AN, Aikawa E, et al. Dual channel optical tomographic imaging of leukocyte recruitment and protease activity in the healing myocardial infarct. Circ Res. 2007; 100: 1218-25. doi:01.RES.0000265064.46075.31 [pii]
10.1161/01.RES.0000265064.46075.31.
5. Ale A, Schulz RB, Sarantopoulos A, Ntziachristos V. Imaging performance of a hybrid x-ray computed tomography-fluorescence molecular tomography system using priors. Med Phys. 37: 1976-86.
6. Ale A, Ermolayev V, Herzog E, Cohrs C, de Angelis MH, Ntziachristos V. FMT-XCT: in vivo animal studies with hybrid fluorescence molecular tomography-X-ray computed tomography. Nat Methods. doi:nmeth.2014 [pii]
10.1038/nmeth.2014.
7. Sarantopoulos A, Themelis G, Ntziachristos V. Imaging the bio-distribution of fluorescent probes using multispectral epi-illumination cryoslicing imaging. Mol Imaging Biol. 13: 874-85. doi:10.1007/s11307-010-0416-8.
8. Christen T, Nahrendorf M, Wildgruber M, Swirski FK, Aikawa E, Waterman P, et al. Molecular imaging of innate immune cell function in transplant rejection. Circulation. 2009; 119: 1925-32. doi:CIRCULATIONAHA.108.796888 [pii]
10.1161/CIRCULATIONAHA.108.796888.
9. Walsh S, Ponten A, Fleischmann BK, Jovinge S. Cardiomyocyte cell cycle control and growth estimation in vivo--an analysis based on cardiomyocyte nuclei. Cardiovasc Res. 86: 365-73. doi:cvq005 [pii]
10.1093/cvr/cvq005.

III) Supplementary Figures

Figure S1

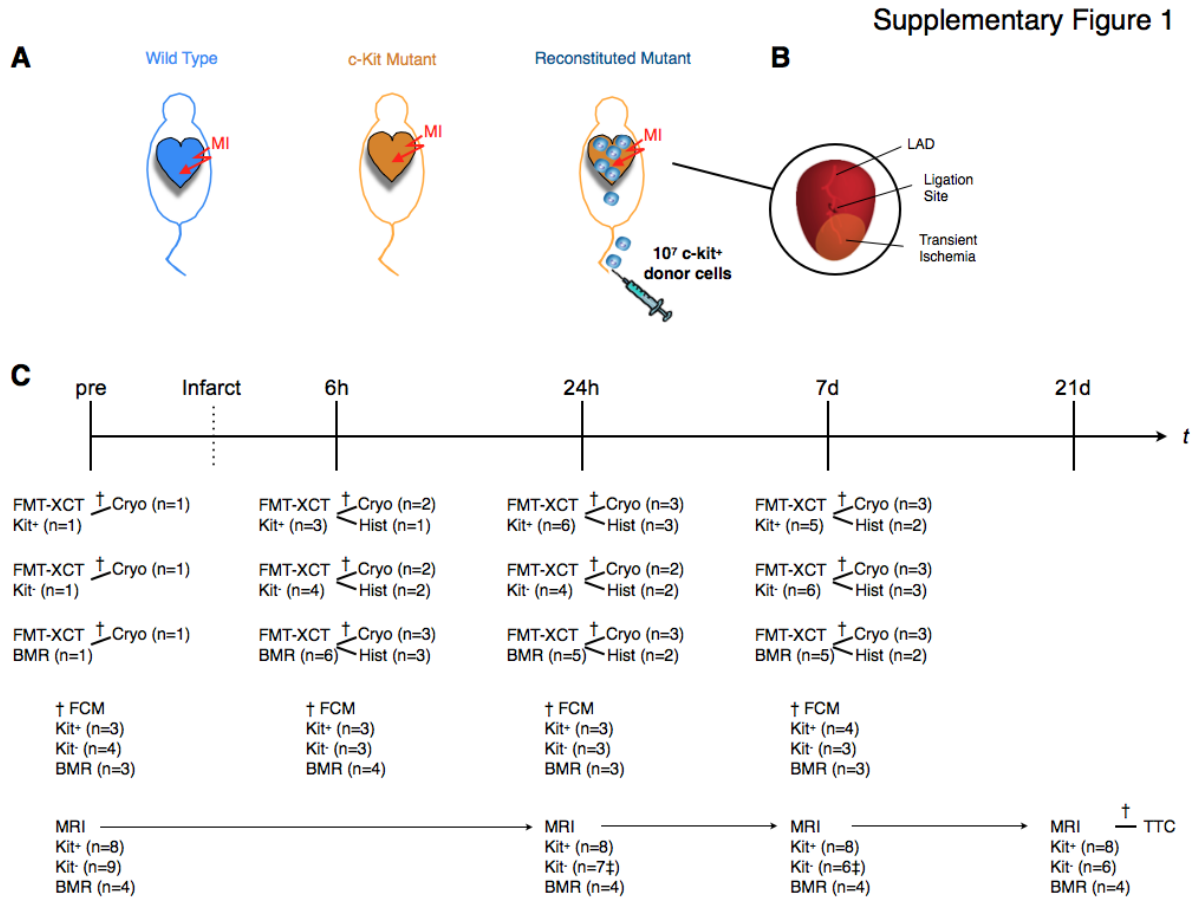

Study design. (A) Studied groups consisted of $Kit^{+/+}$ mice (wild-type, control), Kit^{W}/Kit^{W-v} mice and Kit^{W}/Kit^{W-v} mice reconstituted with 10^7 fresh bone marrow cells from $Kit^{+/+}$ donors. (B) Transient myocardial ischemia is induced via ligation of the left anterior descending artery (LAD) for 30 minutes followed by reperfusion.

(C) Schematic of the study protocol: Animals from the three different groups were studied at various time points by *in-vivo* FMT-XCT imaging followed by sacrifice for *ex-vivo* analysis by Cryoslicing and Histology/Fluorescence Microscopy. An additional group of animals was studied by flow cytometry at each time point. A subgroup of mice was followed over time by cardiac MRI for assessment of heart function.

Animal Groups: Kit^{+} = Kit^{+}/Kit^{+}, Kit^{-} = $Kit^{W}/Kit^{W\text{-}v}$, BMR = $Kit^{+/+}$ BM $\rightarrow$ $Kit^{W}/Kit^{W\text{-}v}$, Cryo=Cryoslicing, Hist=Histology/Fluorescence Microscopy, FCM = Flow Cytometry, † = sacrifice of animal at the given time point, ‡ = death of animal during experiments.

Figure S2

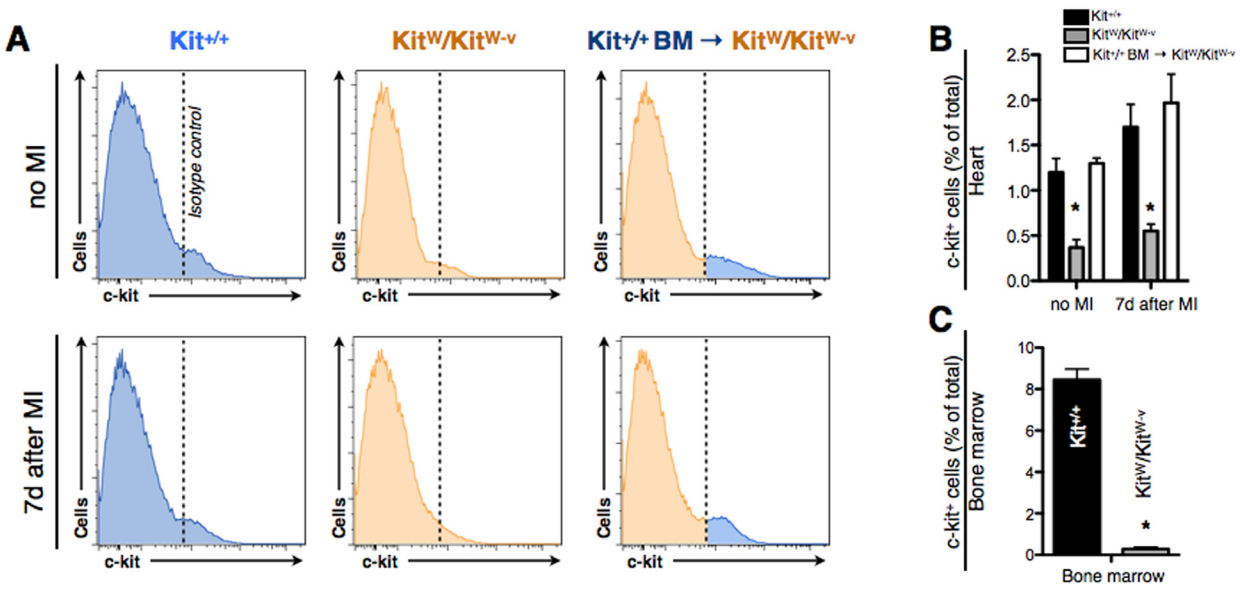

After bone marrow reconstitution c-kit+ cells repopulate the heart both in naïve mice without myocardial infarction as well as post MI. (A) Representative flow cytometry histograms of non-infarcted healthy hearts (first row) and infarcted hearts (second row, post-operative day 7) demonstrate virtual absence of c-kit$^+$ cells within the hearts of *Kit^W/Kit^{W-v}* mice, while reconstitution of *Kit^W/Kit^{W-v}* mice leads to successful repopulation of the heart with a c-kit$^+$ population ~8 weeks after bone marrow reconstitution (n=3-4 mice for healthy and infarcted group from two different experiments). Dotted lines indicate border between positive and negative staining using isotype control. Panel (B) shows quantification of c-kit$^+$ cells in the heart after BMC therapy. In *Kit^W/Kit^{W-v}* mice c-kit$^+$ cells are almost absent within the heart, while the amount of c-kit$^+$ cells in reconstituted mice is significantly increased ($p<0.01$, 2-way ANOVA followed by Bonferroni post test). The percentage of c-kit$^+$ cells within the heart is comparable between wild-type *Kit$^{+/+}$* and reconstituted *Kit$^{+/+}$* BM → *Kit^W/Kit^{W-v}* mice (p=ns). After myocardial infarction the percentage of c-kit$^+$ cells is slightly increased in wild-type and reconstituted animals compared to the naïve

status without MI (p=0.014, 2-way ANOVA). Panel (C) shows percentage of c-kit^{+} cells within the bone marrow of wild-type *Kit*$^{+/+}$ and *Kit*^{W}/*Kit*$^{W-v}$ mice (n=6 in each group). A mean of 8.5 ± 0.7% of BM cells stained positive for c-kit within the cell suspension of *Kit*$^{+/+}$ mice, which was used for cell therapy of *Kit*^{W}/*Kit*$^{W-v}$ mice. *P <0.05.

IV) Supplementary Tables

Table S1

	Bone	Heart	Lung	Mixed Tissue*
Absorption coefficient μ_a (cm^{-1})	0.2	0.35	0.25	0.3
Reduced scattering coefficient μ_s‘ (cm^{-1})	15	17.5	27.5	15

*mixed tissue = muscle, fat and other soft tissue

Table S2

Statistical analysis of differences in cardiac functional parameters of time after onset of myocardial infarction (referring to the Panels D-H in Figure 5).

SV		$Kit^{+/+}$	Kit^{W}/Kit^{W-v}	*$Kit^{+/+}$* BM → *Kit^{W}/Kit^{W-v}*
	General Effect	**	***	**
	pre vs D1	*	ns	ns
	pre vs D7	ns	***	*
	pre vs D21	**	***	**
	D1 vs D7	ns	**	ns
	D1 vs D21	ns	***	ns
	D7 vs D21	ns	ns	ns
EF	General Effect	***	***	**
	pre vs D1	**	ns	*
	pre vs D7	***	***	*
	pre vs D21	***	***	**
	D1 vs D7	*	**	ns
	D1 vs D21	*	***	ns
	D7 vs D21	ns	ns	ns
ESV	General Effect	*	***	*
	pre vs D1	ns	ns	ns
	pre vs D7	ns	**	ns
	pre vs D21	*	***	*
	D1 vs D7	ns	ns	ns
	D1 vs D21	ns	***	ns
	D7 vs D21	ns	**	ns
EDV	General Effect	ns	ns	ns
	pre vs D1	ns	ns	ns
	pre vs D7	ns	ns	ns
	pre vs D21	ns	ns	ns
	D1 vs D7	ns	ns	ns
	D1 vs D21	ns	ns	ns
	D7 vs D21	ns	ns	ns
LV mass	General Effect	ns	ns	ns
	pre vs D1	ns	ns	ns
	pre vs D7	ns	ns	ns
	pre vs D21	ns	ns	ns
	D1 vs D7	ns	ns	ns
	D1 vs D21	ns	ns	ns
	D7 vs D21	ns	ns	ns

Statistical analysis was performed by Analysis of Variance followed by Bonferroni post-hoc test for multiple comparisons, as described in the Methods section. SV=Stroke Volume, EF=Ejection Fraction, ESV=End Systolic Volume, EDV=End Diastolic Volume, LV mass= Left Ventricular Mass, *p<0.05, **p<0.01, ***p<0.001, ns=not statistically significant